Journal of Membrane Science 341 (2009) 84–95

Contents lists available at ScienceDirect

Journal of Membrane Science

journal homepage: www.elsevier.com/locate/memsci

Influence of phenoxy-terminated short-chain pendant groups on gas transport properties of cross-linked poly(ethylene oxide) copolymers

Victor A. Kusuma [a], Scott Matteucci [a,1], Benny D. Freeman [a,*], Michael K. Danquah [b], Douglass S. Kalika [b]

[a] Center for Energy and Environmental Resources, Department of Chemical Engineering, The University of Texas at Austin, Austin, TX 78758, USA
[b] Department of Chemical and Materials Engineering, University of Kentucky, Lexington, KY 40506-0046, USA

ARTICLE INFO

Article history:
Received 21 February 2009
Received in revised form 8 May 2009
Accepted 27 May 2009
Available online 6 June 2009

Keywords:
Cross-linked poly(ethylene oxide)
Chain mobility
Light gas separation
Fractional free volume
Structure/property relationship

ABSTRACT

Gas transport properties of rubbery cross-linked poly(ethylene oxide) films containing short phenoxy-terminated pendant chains are reported. Poly(ethylene glycol) diacrylate (PEGDA) was UV-polymerized with poly(ethylene glycol) phenyl ether acrylate co-monomers of two different ethylene oxide repeat unit lengths: $n=2$ (DEGPEA) and $n=4$ (PEGPEA). Although fractional free volume increased with increasing co-monomer concentration, gas permeability did not rise accordingly. For instance, while *FFV* increased from 0.120 to 0.135 in both series of copolymers, CO_2 permeability went from 110 to 35 barrer (DEGPEA) or to 100 barrer (PEGPEA). At the same time, glass transition temperature increased from −37 to −12 °C (DEGPEA) or to −28 °C (PEGPEA). The observed decrease in chain mobility with phenoxy-terminated co-monomer content indicated by increasing glass–rubber transition temperature apparently had a stronger influence on gas transport properties than the increase in fractional free volume.

1. Introduction

Selective removal of acid gases such as carbon dioxide and hydrogen sulfide from other light gases and hydrocarbons is of considerable industrial interest, and novel high performance membrane materials are needed for membrane modules to compete economically with established processes, such as absorption, in achieving this goal [1]. Among the membrane materials studied for this purpose is the cross-linked poly(ethylene oxide) (XLPEO) family of copolymers [2–10]. These materials are attractive due to the high concentration of polar ether oxygen groups that they contain, which interact favorably with acid gas components, increasing their solubility in the polymer [2] and boosting overall permeability and selectivity over other light gases [11,12]. Examples of separation applications for this family of materials are natural gas sweetening [6], reverse-selective hydrogen purification [7], carbon dioxide sequestration [13,14], and modified atmospheric packaging [15]. XLPEO polymers can be obtained by free-radical photopolymerization of acrylate monomers containing uninterrupted runs of poly(ethylene oxide) (PEO); by limiting the length of the ethylene oxide segments, crystallization is eliminated, leading to fully amorphous networks [4].

Modification of XLPEO network structure via strategic copolymerization can be used to vary transport properties [8,9,13,16]. In an earlier study, PEGDA was copolymerized with one of two monoacrylate co-monomers with similar chemical composition: poly(ethylene glycol) methyl ether acrylate (PEGMEA, containing 8 ethylene oxide repeat units) or poly(ethylene glycol) acrylate (PEGA, containing 7 ethylene oxide repeat units) [8]. Despite the similarity in ethylene oxide content, copolymerization of PEGDA with PEGMEA significantly increased XLPEO gas permeability, while this was not true for copolymerization with PEGA. For instance, CO_2 permeability (35 °C) increased from 110 to 510 barrer with addition of 90 wt% PEGMEA to PEGDA. The difference in gas permeability among the two copolymer formulations was attributed to the terminal functional group of the co-monomer: the $-OCH_3$ terminated PEGMEA branches acted to increase local free volume, while the ability of the –OH terminated PEGA branches to do the same was apparently suppressed by hydrogen bonding between the hydroxyl end group and the surrounding polar network [8,16]. In another study on XLPEO copolymer networks, ethoxy ($-OC_2H_5$) terminal groups were found to be potentially even more effective than $-OCH_3$ terminal groups in increasing gas permeability [9]. Further permeability increase in XLPEO seems achievable by introducing bulky, non-polar, non-interacting terminal groups into the copolymer networks to expand local free volume and increase overall polymer fractional free volume (*FFV*). To assess this hypothesis, we report the physical and transport properties of cross-linked

* Corresponding author at: Center for Energy and Environmental Resources, Department of Chemical Engineering, The University of Texas at Austin, 10100 Burnet Road, Building 133, Austin, TX 78758, USA. Tel.: +1 512 232 2803; fax: +1 512 232 2807.
E-mail address: freeman@che.utexas.edu (B.D. Freeman).
[1] Present address: The Dow Chemical Company, Midland, MI, USA.

0376-7388/$ – see front matter © 2009 Elsevier B.V. All rights reserved.
doi:10.1016/j.memsci.2009.05.043

Table 1
Chemical structures of XLPEO precursors considered in this study. PEGDA is the cross-linker. DEGEEA, DEGPEA and PEGPEA are the principal co-monomers (highlighted in boldface). References for previous studies involving the PEGDA/co-monomer systems are given where applicable.

Name (EO wt%)	Figure symbol	Structure
PEGDA (82%)	N/A	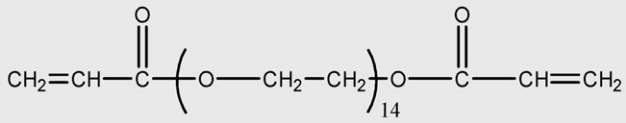
DEGEEA (47%) [32]	▼	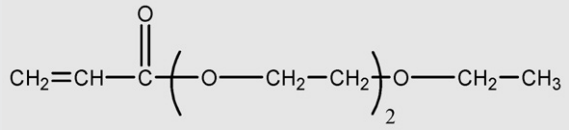
DEGPEA (37%)	□	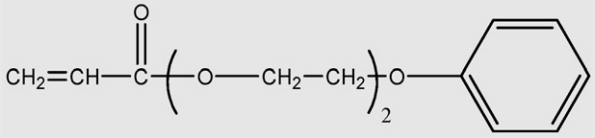
PEGPEA (54%)	○	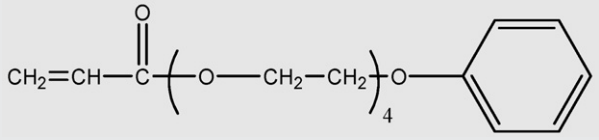
PEGMEA (81%) [6–8,10,16]	◊	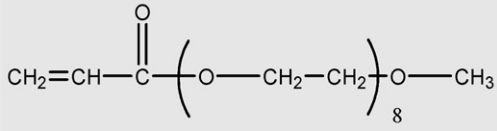
PEGA (81%) [8,10,16]	●	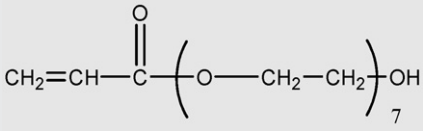
2-EEA (31%) [9]	△	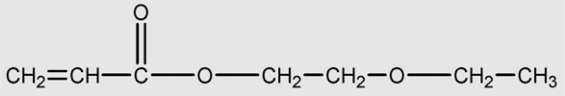

PEGDA prepared with two phenoxy-terminated co-monomers of different chain lengths. PEGDA copolymers prepared with a flexible, ethoxy-terminated co-monomer of comparable length are explored for comparison.

The two phenoxy-terminated co-monomers are di(ethylene glycol) phenyl ether acrylate (DEGPEA) and poly(ethylene glycol) phenyl ether acrylate ($n = 4$) (PEGPEA), containing 37 wt% EO and 54 wt% EO, respectively. The ethoxy-terminated co-monomer is di(ethylene glycol) ethyl ether acrylate (DEGEEA); like DEGPEA, it contains two ethylene oxide moieties per monomer. In DEGEEA, the concentration of ethylene oxide (47 wt% EO) is higher than that of the ethoxy-terminated co-monomer studied previously (2-ethoxyethyl acrylate (2-EEA); 31 wt% EO [9]). Chemical structures are given in Table 1, and a schematic of XLPEO synthesized from these co-monomers is provided in Fig. 1. Characterization of the as-prepared copolymer networks included bulk density measurement for the estimation of fractional free volume, as well as thermal analysis studies for the elucidation of the glass transition and overall polymer chain mobility. Transport properties of the corresponding copolymer networks were established based on experimental determination of pure gas permeability (CO_2, CH_4, H_2, O_2 and N_2) and pure gas solubility (CO_2 and CH_4) at 35 °C.

2. Background

The gas permeability is defined as [17]:

$$P_A \equiv \frac{N_A \cdot l}{f_2 - f_1} \quad (1)$$

where N_A is the steady state gas flux through the film, l is the film thickness, and f_2 and f_1 are the upstream and downstream fugacities of gas A, respectively. Fugacity is used instead of pressure to account for non-ideal gas phase behavior [3], which can be significant for some penetrants (such as carbon dioxide) at high pressure, and all fugacity values were calculated from the virial equation of state using literature parameters [18]. The transport of gases through a dense polymeric film is often described by the solution-diffusion mechanism [19]. Assuming that the process obeys Fick's law and the downstream fugacity is much less than the upstream fugacity, the permeability is given by [19]:

$$P_A = D_A \times S_A \quad (2)$$

where P_A is the permeability of a polymer to a gas A, S_A is the solubility coefficient (defined as the ratio of gas concentration in the polymer at the upstream face of the membrane to the fugacity of

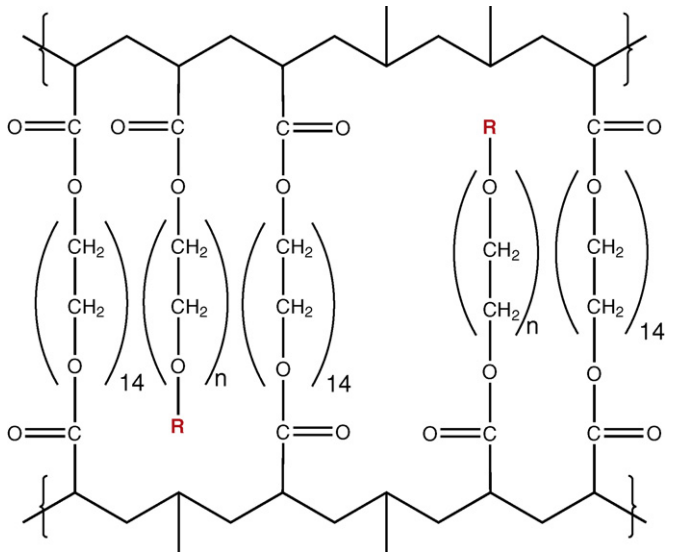

Fig. 1. Scheme of representative network elements in XLPEO, with **R** representing the functional end-group of the monoacrylate co-monomer (**R** = CH_2CH_3 for DEGEEA, C_6H_5 for DEGPEA and PEGPEA) and n representing the average number of ethylene oxide group repeat units (n = 2 for DEGEEA and DEGPEA, 4 for PEGPEA).

the gas in the gas phase contiguous to the upstream face of the membrane), and D_A is the average effective diffusivity in the film.

The ideal selectivity of a polymer film for gas A over gas B is the ratio of their pure gas permeabilities. This ratio can be further described in terms of diffusivity and solubility ratios [12]:

$$\alpha_{A/B} = \frac{P_A}{P_B} = \left[\frac{D_A}{D_B}\right]\left[\frac{S_A}{S_B}\right] \tag{3}$$

where D_A/D_B is the diffusivity selectivity, which is influenced by the size difference between the penetrant molecules and the size-sieving ability of the polymer matrix, and S_A/S_B is the solubility selectivity, which is controlled by the penetrants' condensability and relative affinity for the polymer matrix [12]. Separation in rubbery polymers is typically dominated by solubility selectivity due to their weak size-sieving character [20]; this effect is evident in XLPEO [8,9].

Free volume has been widely used to rationalize the relationship between polymer structure (i.e., chain packing) and gas transport properties [21]. Among the many free volume models proposed, the Fujita-modified Cohen–Turnbull model [22] has been used to relate free volume and gas diffusivity in XLPEO [5,10]:

$$D_A = A_D \exp\left(-\frac{B}{FFV}\right) \tag{4}$$

where A_D is a pre-exponential factor, B is a constant that depends on penetrant size, and FFV is the fractional free volume in the polymer. Generally, diffusivity increases with increasing FFV. Combining Eqs. (2) and (4) yields the following expression for permeability:

$$P_A = A_P \exp\left(-\frac{B}{FFV}\right) \tag{5}$$

where A_P is a pre-exponential factor that is equal to A_D multiplied by the solubility of penetrant A in the polymer, S_A. Direct correlation of permeability and free volume is possible when S_A exhibits little variation with FFV.

FFV is commonly used to characterize the efficiency of chain packing and the amount of free space available for gas permeation in the polymer [23]:

$$FFV = \frac{v - v_0}{v} \tag{6}$$

where v is the specific volume of the amorphous polymer at the temperature of interest (obtained from density measurements), and v_0 is the specific occupied volume at 0 K calculated using the Bondi's group contribution method, estimated as 1.3 times the van der Waals volume by van Krevelen [24]. Further details on the free volume calculation method of XLPEO were given in a previous study [9].

For the PEGDA/PEGMEA network, FFV was correlated with the glass transition temperature by Lin and Freeman [2] as follows [25]:

$$FFV = FFV(T_g) + \alpha_r(T - T_g) \tag{7}$$

where $FFV(T_g)$ is the apparent fractional free volume at T_g, and α_r is the thermal expansion coefficient of the fractional free volume. The parameters for PEGDA/PEGMEA are as follows: $FFV(T_g)$ is 0.055 ± 0.001, and α_r is $(8.4 \pm 2.6) \times 10^{-4}\,K^{-1}$ [2,5]. This correlation suggests a direct relationship between overall polymer chain mobility (indicated by T_g) and free volume, on the basis that, in these particular polymers, compositions containing more flexible chains tend to have higher free volume. The result is an observed decrease in T_g of approximately 25 °C with increasing PEGMEA content across the copolymer series [2]. However, these parameters are not universal for all PEGDA-based copolymers [9]. Copolymerizing PEGDA with short-chain 2-ethoxyethyl acrylate (2-EEA), for instance, increases free volume due to the expansion effect of the ethoxy-terminated 2-EEA branch ends. At the same time, the short branches impart stiffness to the main network backbone by potentially hindering chain motion. The result is a substantial increase in polymer fractional free volume, but virtually no change in T_g [9].

3. Experimental

3.1. Materials

Poly(ethylene glycol) diacrylate (PEGDA; nominal M_w 700 g/mol) was obtained from Aldrich Chemical Company, Milwaukee, WI. The molecular weight and polydispersity were characterized previously [4]. This PEGDA has a number-average molecular weight of 743 Da (by NMR), consistent with a monomeric repeat value of $n \sim 14$. The acrylate co-monomers, di(ethylene glycol) ethyl ether acrylate (DEGEEA; M_w = 118, technical grade), di(ethylene glycol) phenyl ether acrylate (DEGPEA, listed in the catalog as poly(ethylene glycol) phenyl ether acrylate (n = 2); $M_w \sim 236$) and poly(ethylene glycol) phenyl ether acrylate (n = 4) (PEGPEA; $M_w \sim 324$), were also obtained from Aldrich, as was 1-hydroxyl-cyclohexyl phenyl ketone (HCPK; purity 99%) photoinitiator. All reagents were used as received. All gases were obtained from Airgas Southwest Inc. (Corpus Christi, TX), with purity of at least 99.9% (except for methane: 99.0%), and they were used as received.

3.2. Film preparation

Films were prepared via UV photopolymerization using a procedure similar to that described for other PEGDA copolymers [8,9]. Liquid prepolymerization mixtures were prepared with the desired proportions of PEGDA cross-linker and an acrylate co-monomer, as well as 0.1 wt% HCPK photoinitiator. This mixture was sandwiched between parallel quartz plates, separated by spacers, and then exposed to 312 nm light for 90 s at 3 mW/cm^2 in a UV cross-linking chamber (Spectrolinker XL-1000, Spectronics Corporation, Westbury, NY). Film thicknesses were between 350 and 550 μm for transport measurements, ~1 mm for the dynamic mechanical specimens, and ~350 μm for the dielectric specimens. The exact thickness was determined within ±1 μm using a digital micrometer (ABSOLUTE Digimatic series 547, Mitutoyo Corp., Japan). Before further use, the resulting freestanding films were extracted for 5

Table 2
Physical properties of PEGDA/DEGEEA, PEGDA/DEGPEA and PEGDA/PEGPEA copolymers.

Co-monomer	PEGDA mol%	PEGDA wt%	T_g (°C)	ρ_P (g/cm^3)	*FFV*
–	100	100	−37 ± 1	1.190 ± 0.004	0.120 ± 0.003
DEGEEA	80	94	−38 ± 1	1.184 ± 0.004	0.123 ± 0.003
	60	85	−39 ± 1	1.180 ± 0.004	0.126 ± 0.003
	40	71	−41 ± 1	1.171 ± 0.004	0.131 ± 0.003
	20	48	−44 ± 1	1.159 ± 0.004	0.139 ± 0.003
	10	29	−46 ± 1	1.148 ± 0.004	0.146 ± 0.003
DEGPEA	80	92	−35 ± 1	1.188 ± 0.004	0.123 ± 0.003
	60	82	−32 ± 1	1.193 ± 0.004	0.122 ± 0.003
	40	66	−29 ± 1	1.195 ± 0.004	0.126 ± 0.002
	20	43	−23 ± 1	1.199 ± 0.002	0.129 ± 0.002
	10	25	−17 ± 1	1.201 ± 0.004	0.133 ± 0.003
	0	0	−12 ± 1	1.209 ± 0.003	0.135 ± 0.002
PEGPEA	80	90	−37 ± 1	1.185 ± 0.002	0.124 ± 0.002
	60	77	−35 ± 1	1.186 ± 0.003	0.125 ± 0.003
	40	59	−33 ± 1	1.188 ± 0.004	0.126 ± 0.003
	20	35	−31 ± 1	1.190 ± 0.004	0.128 ± 0.003
	0	0	−28 ± 1	1.186 ± 0.004	0.135 ± 0.003

days in ultrapure water (Milli-Q water purification system, Millipore Corporation, Bedford, MA), with water changed daily. Films so treated consisted of three-dimensional networks (gel) and a negligible amount of low molecular weight polymer (sol) that was not bound to the network [4]. Afterward, the films were dried in air at ambient conditions prior to measurements.

3.3. Fourier transform infrared spectroscopy

Attenuated total reflection Fourier transform infrared spectroscopy (FTIR-ATR) analysis was performed using a Thermo-Nicolet (Madison, WI) Nexus 470 spectrometer, with each average spectrum obtained from 128 scans at 1 cm^{-1} resolution. The conversion of acrylate double bonds due to polymerization led to a decrease in sharp peaks at 810 cm^{-1} (ascribed to the twisting vibration of the acrylic CH_2=CH bond), at 1410 cm^{-1} (deformation of the CH_2=CH bond) and at 1190 cm^{-1} (acrylic C=O bond) [8]. The cross-linking method used for copolymer mixtures with PEGDA of this molecular weight produced essentially complete reaction confirmed by the total disappearance of the acrylate double bond signature peaks (spectra not shown) [8,9,26]. Weight loss due to the water extraction step was considered negligible.

3.4. Film density

The density of the dry polymer films was determined by hydrostatic weighing using a Mettler Toledo balance model AG204 (Switzerland) and a density determination kit. The density was determined using the difference between the polymer mass in air and in an auxiliary liquid, *n*-heptane. The sample preparation method described below follows that of the previous study [9]. The polymer samples were first degassed overnight in a vacuum oven at ambient temperature, then purged and transferred under dry nitrogen into the balance prior to density determination. The time taken for density measurements was much less than the timescale of vapor re-sorption into the polymer as determined from sorption experiments, and thus the density measurements were performed at ambient conditions without nitrogen blanketing.

3.5. Thermal analysis

Thermal transitions were determined using a TA Instruments (New Castle, DE) Q100 differential scanning calorimeter (DSC). TA Instruments indicates that the accuracy in the temperature reported by this instrument is ±0.1 °C. Samples (~10 mg) were initially quenched to −90 °C and scanned twice at a heating rate of 10 °C/min up to 150 °C under a dry N_2 purge flow rate of 50 ml/min. The glass transition temperature (T_g) was taken as the midpoint of the heat capacity step change that appeared in the second heating scan. No crystallization peaks were observed for any of the networks examined in this study.

Dynamic mechanical thermal analysis was performed using a Polymer Laboratories DMTA (Amherst, MA) operating in single cantilever bending geometry. Films (thickness ~1.0 mm) were held under vacuum at room temperature for at least 24 h prior to measurement. The sample mounting procedures were designed to minimize exposure to ambient moisture. Storage modulus (E') and loss tangent ($\tan\delta$) were measured at a heating rate of 1 °C/min with test frequencies of 0.1, 1, and 10 Hz. All experiments were carried out under an inert (N_2) atmosphere.

Dielectric measurements were conducted using the Novocontrol Broadband Dielectric Spectrometer (Hundsangen, Germany). Dielectric constant (ε') and loss (ε'') were recorded in the frequency domain (0.1 Hz to 1 MHz) at isothermal intervals from −150 to 50 °C. Concentric silver electrodes were applied to each sample film (thickness ~350 μm) using a VEECO (Plainview, NY) thermal evaporation system and all samples were dried under vacuum at room temperature prior to measurement. Dispersion spectra were analyzed using the Novocontrol WINFIT software to establish relaxation time (τ_{MAX}) as a function of temperature for both the sub-glass and glass rubber relaxation processes.

3.6. Permeation and sorption measurements

Pure gas permeability values were determined using a constant volume/variable pressure apparatus [27,28]. The gas flux was measured from the pressure rise in a pre-evacuated downstream vessel of known volume when pure gas was applied on the upstream side at a known high pressure (in this case, 3–15 atm); the corresponding pure gas permeability was calculated according to Eq. (1). The polymer samples were partially masked with impermeable aluminum tape that was glued with epoxy to the upstream face of the film. This masking procedure was used to accurately define the surface area available for mass transport and to prevent damage to the films during permeation testing. Gas solubility coefficients for each polymer sample were determined using a dual-volume, dual-transducer apparatus based on the barometric pressure-decay method [29] as described previously [9]. All permeability and solu-

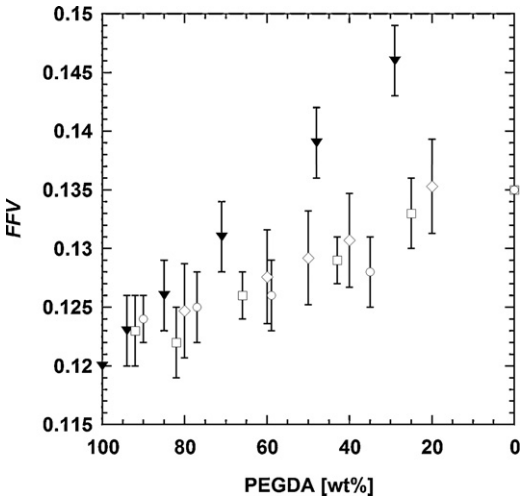

Fig. 2. Fractional free volume of PEGDA copolymers as a function of PEGDA content in the prepolymer solution. The co-monomers are (▼) DEGEEA, (◊) PEGMEA, (□) DEGPEA and (○) PEGPEA. Free volume for PEGMEA was calculated using density data measured for this study according to assumptions detailed in Ref. [9].

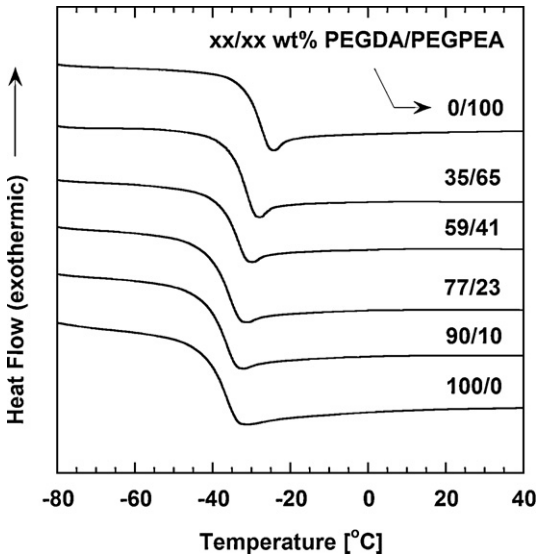

Fig. 3. Second scan DSC thermograms for PEGDA/PEGPEA copolymers. The heating rate was 10 °C/min. The thermograms have been displaced vertically for clarity.

bility experiments were performed at 35 °C, with errors calculated based on standard propagation of error method [30].

4. Results and discussion

4.1. Fractional free volume and chain mobility

Density, glass transition temperature and fractional free volume (*FFV*) data for the copolymer films prepared in this study are presented in Table 2. Increasing the amount of phenoxy-terminated ($-OC_6H_5$) co-monomers (DEGPEA or PEGPEA) in the cross-linked PEGDA networks leads to a systematic increase in *FFV*. Similar to the methoxy- or ethoxy-terminated monomers, such as PEGMEA [8], 2-EEA [9] and DEGEEA (cf. Table 1), the bulky, non-polar phenoxy groups at the end of the flexible pendant chains appear to be responsible for the observed increase in local free volume in the networks. As illustrated in Fig. 2, the increases in *FFV* across the PEGDA/DEGPEA and PEGDA/PEGPEA network series appear to be similar, despite the difference in pendant chain length. However, the *FFV* increases are lower than the trend observed for the PEGDA/DEGEEA networks.

The glass transition temperature provides an indication of the overall copolymer chain mobility. Representative DSC scans for the PEGDA/PEGPEA copolymers are shown in Fig. 3. Fig. 4 compares the glass transition temperatures of the PEGDA/DEGPEA and PEGDA/PEGPEA copolymers to those of the PEGDA/DEGEEA, PEGDA/2-EEA [9] and PEGDA/PEGMEA [8] networks. The glass transition temperatures follow a random copolymer model as given by the Fox equation [31]:

$$\frac{1}{T_g} = \sum_i \frac{w_i}{T_{gi}} \tag{8}$$

where w_i is the weight fraction of each component in the prepolymer solution, and T_{gi} is the glass transition temperature of the pure polymerized component, as measured experimentally using DSC. For the XLPEGDA copolymer networks containing phenoxy-terminated side chains, an increase in glass transition temperature is observed with increasing co-monomer content, the effect being stronger in copolymers containing shorter DEGPEA pendant groups. The increase in T_g is presumably due to the bulky character of the phenoxy terminal group, which introduces considerable steric hindrance to segmental motions associated with the glass transition. The glass transition temperatures of the DEGEEA-based copolymers, in contrast, decrease with increasing co-monomer content, and fall between those of PEGDA/2-EEA and PEGDA/PEGMEA. This result appears to be primarily a reflection of side chain length, as determined by the number of flexible repeat units within the respective co-monomers [31].

While changes in *FFV* can be correlated with overall polymer chain mobility and T_g (see Eq. (7)), such correlations are not necessarily universal across various copolymer series. Both the length of the co-monomer side chains and the nature of the side chain terminal groups can significantly affect the glass transition temperature and free volume characteristics of the resulting networks [8,9,16,32]. *FFV*-T_g correlations for the copolymers considered in this study are shown in Fig. 5. In all cases, the introduction of the PEG-based side chains produces an increase in *FFV* with increasing co-monomer content. For PEGDA/DEGEEA, the relatively flexible, compact DEGEEA pendants lead to a progressive reduction in T_g

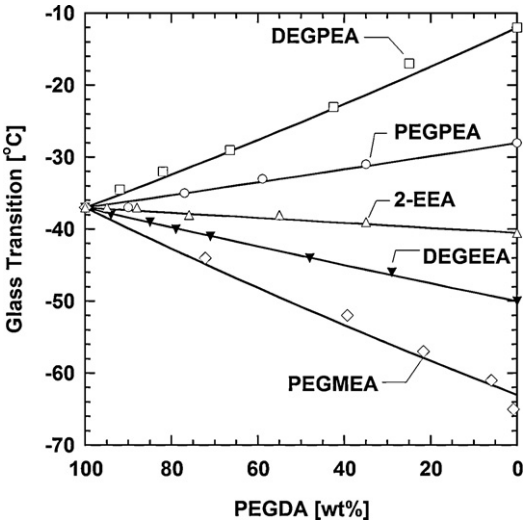

Fig. 4. Effect of PEGDA content in the prepolymer solution on glass transition temperature determined by DSC. The co-monomers are (Δ) 2-EEA, (▼) DEGEEA, (◊) PEGMEA, (□) DEGPEA and (○) PEGPEA. The model lines are drawn based on Eq. (8) (Fox equation). Data for PEGMEA are reproduced from Ref. [8], and those for 2-EEA are from Ref. [9]. The uncertainty is ±1 °C.

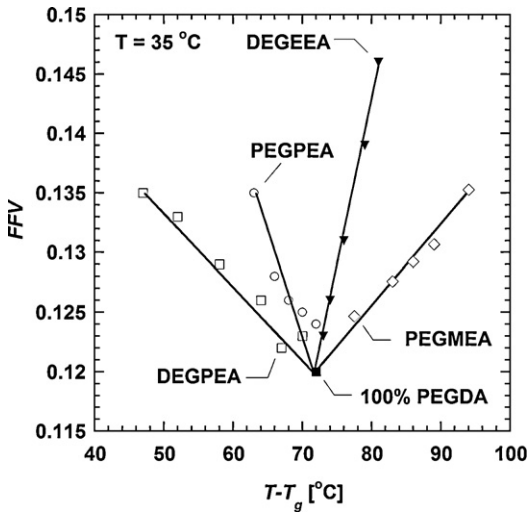

Fig. 5. Fractional free volume of XLPEO vs. ($T - T_g$), where T = 35 °C and T_g is the glass transition temperature of the corresponding copolymer. T_g data are obtained from Fig. 4 and plotted against *FFV* from Fig. 2. (■) 100% PEGDA, (▼) PEGDA/DEGEEA, (◊) PEGDA/PEGMEA, (□) PEGDA/DEGPEA and (○) PEGDA/PEGPEA.

with increasing branch concentration, a trend that is consistent with the results for the PEGDA/PEGMEA series. However, for networks containing the phenoxy-terminated side chains, the steric hindrance introduced by the terminal phenyl group drives T_g upwards with increasing branch content, an effect that is especially pronounced for the shorter DEGPEA pendant, which is spatially more strongly correlated to the network backbone. The outcome is distinct *FFV*-T_g relations that appear to independently reflect the influence of co-monomer repeat length, and the relative bulk and chemical nature of the side chain terminal groups. As such, increased *FFV* in the phenoxy-terminated copolymer series does not reflect increased polymer chain flexibility.

Additional insights into the structure and relaxation properties of the copolymer networks were obtained via dynamic mechanical and dielectric spectroscopy measurements; these results complement detailed dynamic studies on XLPEGDA networks reported previously. Representative dynamic mechanical data for the PEGDA/PEGPEA copolymer series are shown in Fig. 6, and demonstrate the influence of increasing co-monomer content on the glass–rubber relaxation. Similar data for the PEGDA/DEGEEA series were presented earlier [32]. With increasing PEGPEA co-monomer, the glass transition temperature shifts to higher values consistent with the calorimetric results; the associated peak temperatures (T_α, based on peak in tan δ at 1 Hz) are reported in Table 3. The observed increase in relaxation intensity with co-monomer content is primarily a reflection of the stoichiometrically

Table 3
Characteristics of PEGDA/DEGEEA and PEGDA/PEGPEA as determined via dynamic mechanical analysis.

Co-monomer	PEGDA [wt%]	T_α (1 Hz) (°C)	β_{KWW}
–	100	−35	0.30
DEGEEA[a]	80	−36	0.29
	60	−38	0.33
	50	−38	0.32
PEGPEA	80	−32	0.23
	60	−31	0.21
	50	−27	0.20
	40	−27	0.19

Note: T_α [°C] is the dynamic mechanical peak temperature at 1 Hz; β_{KWW} is the Kohlrausch–Williams–Watts distribution parameter [33].
[a] PEGDA/DEGEEA data are taken from [32].

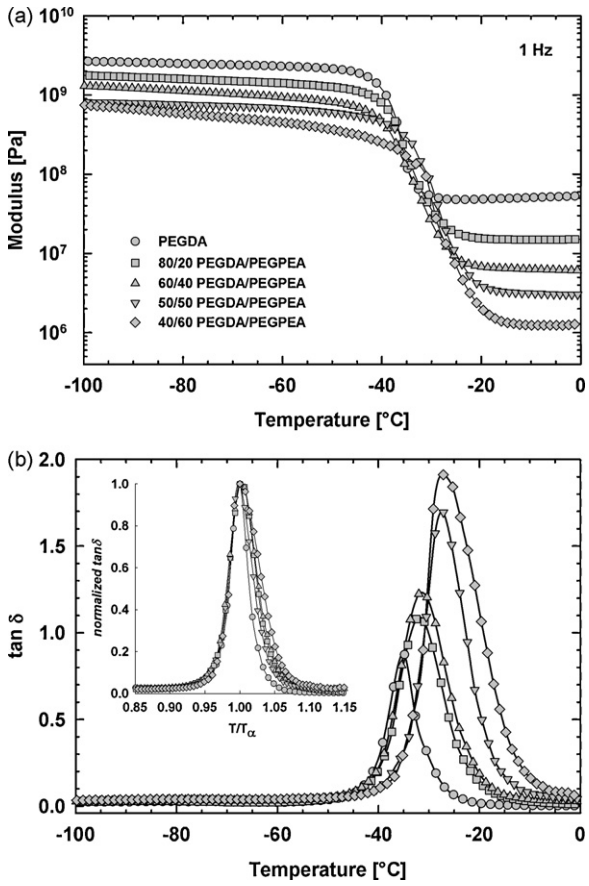

Fig. 6. (a) Dynamic mechanical storage modulus (E') [Pa] and (b) tan δ vs. temperature [°C] for PEGDA/PEGPEA copolymers at 1 Hz; all compositions expressed on a wt% basis. Inset on (b): normalized tan δ vs. T/T_α for PEGDA/PEGPEA copolymers. Symbols are defined in Fig. 6a.

controlled decrease in cross-link density across the copolymer series.

Time–temperature superposition was used to establish storage modulus master curves for each copolymer composition, consistent with prior studies [16,26]. The resulting master curves were fit using the Kohlrausch–Williams–Watts (KWW) stretched-exponential function, with the corresponding exponent designated as β_{KWW} [33]. Values of β_{KWW} can range from 0 to 1, with β_{KWW} = 1 corresponding to a pure Debye relaxation response. The exponent determined for the XLPEGDA homopolymer network, β_{KWW} = 0.30 [26]. Across the highly flexible PEGDA/PEGMEA series, the glass–rubber relaxation was observed to narrow with increasing co-monomer content and correspondingly lower cross-link density [16]. For the PEGDA/PEGPEA series studied here, however, the introduction of bulky side pendants leads to a broadening of the relaxation and a progressive decrease in the β_{KWW} exponent, despite the reduced cross-link constraint associated with increasing co-monomer content (see Table 3). The inset to Fig. 6b (normalized tan δ vs. normalized relaxation temperature) indicates that most of this broadening occurs on the high-temperature side of the glass–rubber relaxation.

Dielectric measurements performed on the PEGDA/PEGPEA copolymers provide information with respect to the intensity and time–temperature behavior of both the sub-glass and glass–rubber relaxations. Dielectric studies on crystalline PEO and the XLPEGDA homopolymer indicate two local sub-glass relaxations (β_1 and β_2), as well as the glass–rubber relaxation (α) with increasing temperature [34]; the influence of co-monomer content on the dielectric dispersion characteristics of various PEGDA copolymers has been

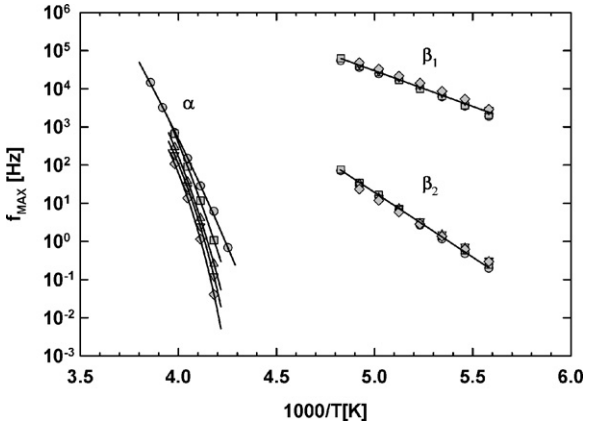

Fig. 7. Arrhenius plot of f_{MAX} [Hz] vs. 1000/T [K] for PEGDA/PEGPEA copolymers based on dielectric measurements; all compositions expressed on a wt% basis. Symbols are defined in Fig. 6a.

reported in detail [32,35]. An Arrhenius plot (f_{MAX} vs. 1000/T) for the PEGDA/PEGPEA copolymers studied here is shown in Fig. 7, where $f_{MAX} = [2\pi\tau_{MAX}]^{-1}$ and τ_{MAX} is the relaxation peak time. For both sub-glass processes, a linear result is obtained, consistent with the localized, essentially non-cooperative character of these relaxations. The data are independent of copolymer composition, with corresponding activation energies identical to the 100% XLPEGDA result: $E_A(\beta_1) = 41$ kJ/mol, and $E_A(\beta_2) = 65$ kJ/mol [34]. This comparison indicates that despite their bulky nature, the presence of the phenoxy-terminated side chains does not alter the time–temperature character of the sub-glass transitions. Across the glass–rubber relaxation, the data indicate a non-Arrhenius process that is cooperative in character, and which can be described by the Williams–Landel–Ferry (WLF) relation (see solid curves in Fig. 7) [36]. The relative position of each copolymer data set reflects the progressive increase in T_g (or relaxation time) with increasing co-monomer content.

The dielectric relaxation response characteristics of the PEGDA/PEGPEA copolymers are similar in many respects to the results obtained for the model PEGDA/PEGMEA series, and are not detailed here in the interest of brevity. For more information regarding the dielectric relaxation behavior of the XLPEGDA copolymers, the reader is referred to Ref. [35].

4.2. Gas transport properties

The permeability of light permanent gases and methane through XLPEO is essentially independent of gas fugacity, due to the low solubility of these gases in XLPEO [3,5,8]. Of the gases considered in this study, only carbon dioxide has high solubility at high fugacity, leading to plasticization of the polymer and higher permeability. Therefore, to compare the permeability values of carbon dioxide with those of the other gases on a consistent basis, the data were interpolated to infinite dilution (i.e., an upstream fugacity of zero) from several measurements performed at various fugacities [9,37]:

$$P_A = P_{A,0}(1 + m_{P,E}\Delta f) = P_{A,0}(1 + m_{P,E}f_2) \quad (9)$$

where $m_{P,E}$ is an adjustable constant at a given temperature, and Δf is the difference between the upstream and downstream fugacity, $\Delta f = f_2 - f_1$. Because the downstream fugacity, f_1, is much less than f_2, Δf can be approximated by f_2. $P_{A,0}$ is the infinite dilution permeability. The order of the gas permeability values in all XLPEO systems, including those in this study, is: $CO_2 > H_2 > O_2 \geq CH_4 > N_2$ [8,9]. Permeability is a function of gas molecule size (as characterized by kinetic diameter), condensability (as characterized by critical temperature) and particularly in the case of CO_2, affinity with the polymer. Among the gases examined here, CO_2 has the highest permeability by virtue of its relatively small size, high condensability and favorable interaction with the polar ether oxygen groups in XLPEO. Methane, which is the largest molecule in the group, displays condensability second only to CO_2 and thus has higher permeability than its size would otherwise indicate.

Fig. 8 presents gas permeability as a function of co-monomer content. The data obey the following random binary copolymer model [38]:

$$\ln P_A = \varphi_1 \ln P_{A,1} + \varphi_2 \ln P_{A,2} \quad (10)$$

where φ_1 and φ_2 are the volume fractions of PEGDA and co-monomer in the polymer, respectively. The volume fractions were estimated as follows: $\varphi_1 = \rho_P w_1/\rho_1$, where w_1 is the weight fraction of PEGDA in the copolymer, ρ_P is the density of the copolymer, and ρ_1 is the density of XLPEO polymerized from 100% PEGDA; $\varphi_2 = 1 - \varphi_1$. Given the relatively small variations in density encountered across each polymer series, the resulting φ_i values are nearly identical to the wt% figures reported in Table 2. $P_{A,1}$ was determined by experimental measurement of 100% PEGDA polymer. For the DEGPEA and PEGPEA series, $P_{A,2}$ was determined by direct experimental measurement of the polymerized acrylate monomer. However, for the DEGEEA series, $P_{A,2}$ could not be determined directly due to a lack of structural integrity for the pure polymerized DEGEEA film. In this case, $P_{A,2}$ was estimated instead by applying Eq. (10) to the sample polymerized with the least amount of PEGDA.

In general, permeability of all gases increases with DEGEEA co-monomer content in XLPEGDA, which is consistent with the results obtained for its shorter analogue, 2-EEA [9], as well as with PEGMEA. According to Eq. (5), permeability should increase as *FFV* increases. Therefore, the observed *FFV* increase with increasing DEGEEA content appears to account for the observed increase in gas permeability. The increase in permeability for light gases other than CO_2 is nearly the same in PEGDA/DEGEEA as in PEGDA/2-EEA and is attributable to the comparable structure of the two short-chain ethoxy-terminated co-monomers, leading to similar *FFV* and gas diffusivity at the same monomer concentrations. DEGEEA, however, contains an additional ethylene oxide group and this ethylene oxide unit results in increased CO_2 affinity with the polymer and, in turn, higher CO_2 permeability in PEGDA/DEGEEA as compared to PEGDA/2-EEA. The CO_2 permeability increase in PEGDA/DEGEEA with increasing co-monomer content nearly matches the increase observed in the PEGDA/PEGMEA system, despite the lower EO content of DEGEEA.

Given the *FFV* increase encountered upon increasing PEGPEA or DEGPEA concentration in the XLPEO networks, which was similar to that encountered in PEGDA/PEGMEA, one might anticipate an increase in gas permeability of these materials. However, this result is not observed. Instead, gas permeability of the PEGDA/PEGPEA series varies little with PEGPEA content, increasing only slightly for penetrants other than CO_2. Gas permeability decreases significantly with addition of the shorter DEGPEA co-monomer. For example, CO_2 permeability decreases from 110 barrer for pure XLPEGDA to 35 barrer for polymerized DEGPEA.

Pure gas ideal selectivity data are presented in Fig. 9. The gas selectivity trends in XLPEO primarily result from the changing gas affinity due to changes in polymer chemical properties (in the case of CO_2), and changes in the size-sieving ability of the polymer due to changes in free volume and chain stiffness [9]. An increase in size-sieving ability favors the transport of gases with smaller kinetic diameter, and can be illustrated by considering the selectivity of permanent gases [7,9]. Selectivity comparisons for the permanent gases (i.e., H_2/N_2 and O_2/N_2) are presented in Fig. 9a. For these gas pairs, any changes in permanent gas selectivity should be due mainly to size differences: H_2 (2.89 Å) vs. N_2 (3.64 Å), and O_2 (3.46 Å) vs. N_2 (3.64 Å) [39]. As shown in Fig. 9a, changes in permanent gas

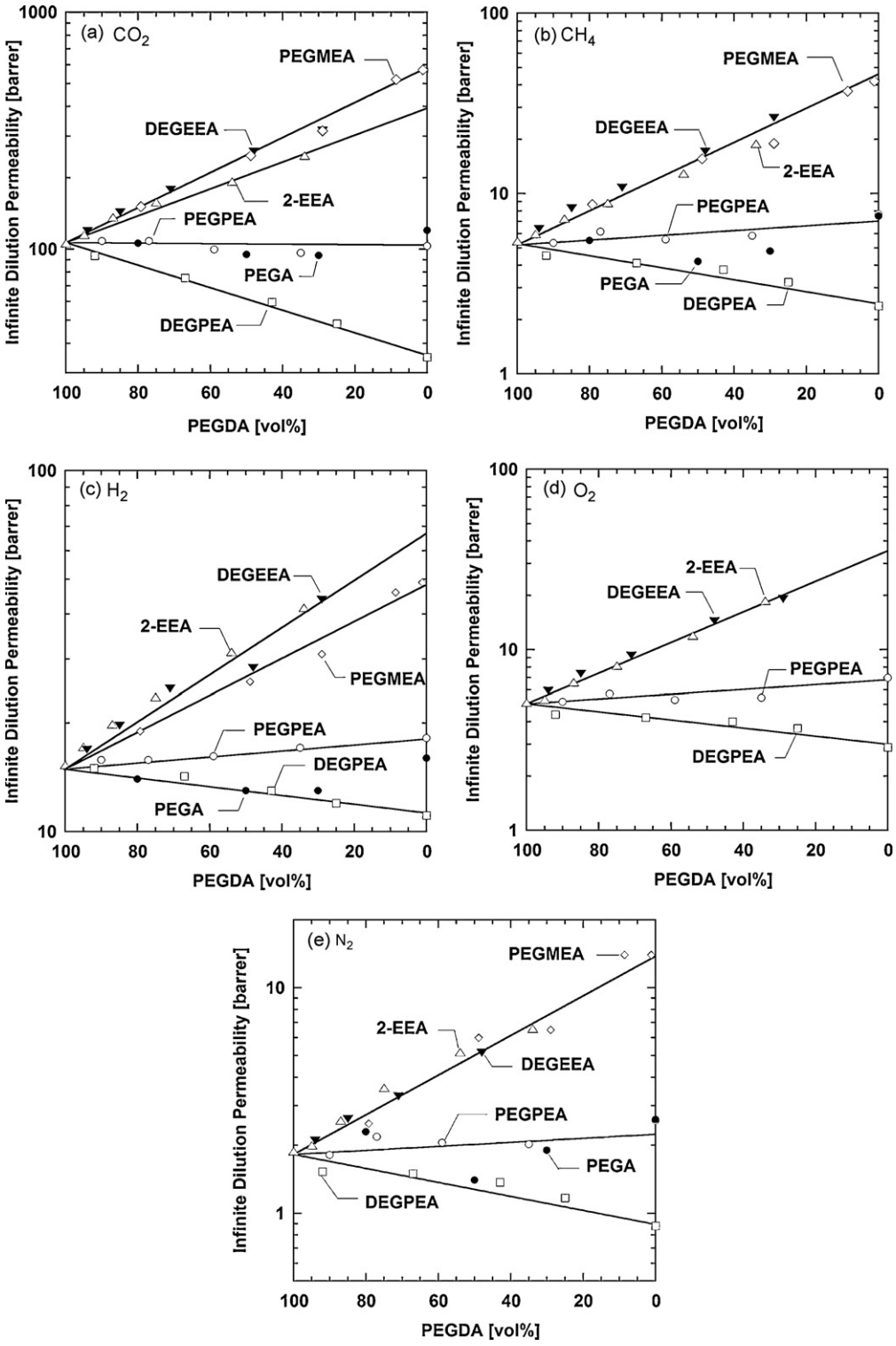

Fig. 8. Effect of PEGDA content on infinite dilution gas permeability at 35 °C. The lines through the data are based on Eq. (10). The gases are (a) CO_2, (b) CH_4, (c) H_2, (d) O_2 and (e) N_2. The co-monomers are (▼) DEGEEA, (◊) PEGMEA, (△) 2-EEA, (□) DEGPEA, (◯) PEGPEA, (●) PEGA. PEGMEA and PEGA data were reproduced from [8] and 2-EEA data from [9]. The average uncertainty is ±6% of the permeability value.

selectivity as a result of changing polymer size-sieving characteristics for PEGDA/DEGEEA, PEGDA/DEGPEA and PEGDA/PEGPEA series are not significant within the measurement uncertainty.

Fig. 9b and c shows selectivity values for CO_2/CH_4 and CO_2/H_2. Across each series, the overall EO content of the network decreases with increased DEGEEA, DEGPEA or PEGPEA concentration. In Fig. 9b, CO_2/CH_4 selectivity generally decreases with increasing co-monomer content regardless of the co-monomer, even the ones containing high EO content such as PEGMEA. As such, the relative affinity of CO_2 and CH_4 for the polymer does not appear to play a significant role in differentiating the selectivity trends for each series. In contrast, H_2 molecules are much smaller and less condensable than CH_4. Apparently, the combined effects of size discrimination, however minimal, and the change in CO_2 affinity for the polymer

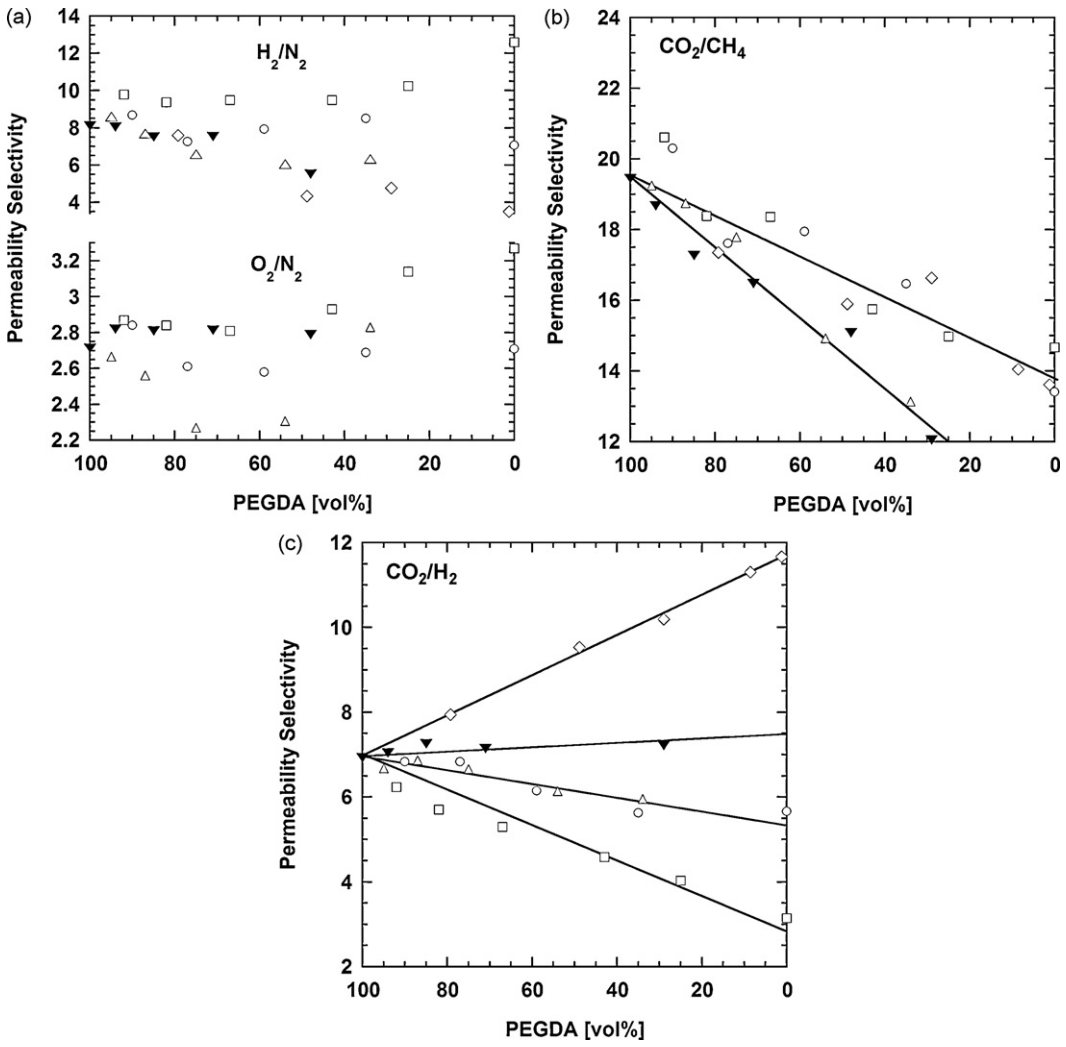

Fig. 9. Effect of PEGDA content on infinite dilution gas selectivity at 35 °C. The solid lines are drawn to guide the eye. The selectivities are (a) H_2/N_2 and O_2/N_2, (b) CO_2/CH_4, and (c) CO_2/H_2. The co-monomers are (▼) DEGEEA, (◊) PEGMEA, (△) 2-EEA, (□) DEGPEA, (◯) PEGPEA. The average uncertainty is ± 8% of the selectivity value.

network compared to H_2 were sufficient to produce more distinct trends in CO_2/H_2 selectivity for the various copolymers, as shown in Fig. 9c.

In order to directly assess CO_2 and CH_4 affinity for the polymer networks, sorption isotherms were obtained by measuring gas uptake in the polymer at equilibrium as a function of fugacity. The isotherms were linear in all cases, so solubility coefficients are reported as Henry's law coefficients [20]. The solubilities of permanent gases in XLPEO were too low to measure. The infinite dilution solubility coefficients are plotted as a function of copolymer composition in Fig. 10, along with data from several copolymer systems studied previously.

The CO_2 solubility coefficients tend to increase with increasing DEGEEA content, consistent with trends previously observed in 2-EEA [9] and PEGMEA [8,40]. Addition of DEGEEA, like 2-EEA, introduces branches with relatively non-polar ends and lower EO content as compared to PEGDA, and thus increasing the amount of DEGEEA tends to lower overall polar content while simultaneously reducing cross-link density. Given the reduction in EO content with increasing DEGEEA, CO_2 solubility would be expected to decrease with increasing DEGEEA concentration [20]. However, as observed in Fig. 10a, the CO_2 solubility coefficients in PEGDA/DEGEEA copolymers increase with increasing DEGEEA content. As DEGEEA concentration increases, the lower polar content in the polymer will lead to a decrease in overall polymer cohesive energy density and a reduction in the energy required to open a gap in the polymer matrix of sufficient size to accommodate a penetrant molecule [9,20]. This reduction in cohesive energy density would be expected to act to increase solubility of all gases, and in the case of CO_2, it is apparently strong enough to counter a lower affinity to CO_2 that presumably accompanies the reduction in polar group content as DEGEEA concentration increases. Additionally, the reduction in cross-link density with increasing DEGEEA content would act to increase solubility as well.

In contrast, the CO_2 solubility in both phenoxy-terminated copolymer systems decreases with increasing co-monomer content. The phenyl terminal groups of the DEGPEA or PEGPEA branches are less polar than the alkoxy end groups on 2-EEA, DEGEEA or PEGMEA. Lower polar content in the PEGDA/DEGPEA and PEGDA/PEGPEA networks, due to lower ethylene oxide content and the addition of phenoxy groups, may be the decisive factor with respect to CO_2 solubility for these series, particularly for PEGDA/DEGPEA (n = 2 EO in side chains). A decrease in CO_2 solubility has also been observed in PEGDA copolymerized with hydroxy-terminated 2-hydroxyethyl acrylate (2-HEA), where strong hydrogen bonds led to enhanced inter-chain interactions, possibly contributing to increased cohesive energy density.

Infinite dilution diffusion coefficients can be calculated from permeability and solubility data using Eq. (2); these results are shown in Fig. 11. As in the other XLPEO systems, the gas diffusivity

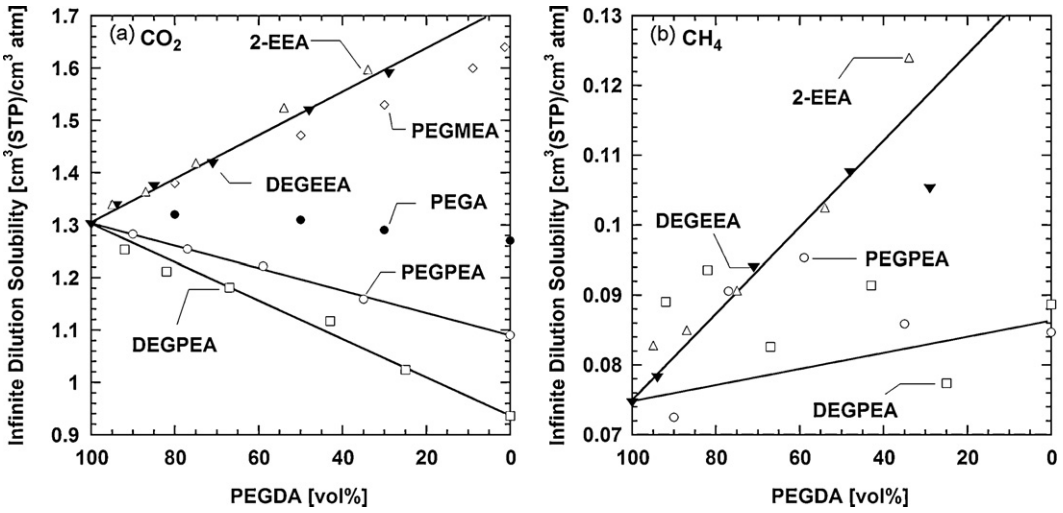

Fig. 10. Effect of PEGDA content on infinite dilution gas solubility at 35 °C, (a) CO_2 and (b) CH_4. The co-monomers are (▼) DEGEEA, (○) PEGPEA and (□) DEGPEA. The lines are drawn to guide the eye. Comparison data with (◊) PEGMEA, (△) 2-EEA, and (●) PEGA are given when available [8,9]. The average uncertainty is ±0.04 cm^3(STP)/cm^3 atm.

follows the trends in permeability to a substantial degree [8,9]. As expected, both CO_2 and CH_4 diffusivity increases with increasing DEGEEA concentration: gas diffusivity tends to be slightly higher in the PEGDA/DEGEEA copolymers than in PEGDA/2-EEA at similar co-monomer content owing to the higher chain mobility (i.e., lower T_g) imparted by the longer, more flexible DEGEEA branches. As shown in Figs. 12 and 13, the permeability and diffusivity coefficients in the PEGDA/DEGEEA series are well-described by the Cohen–Turnbull model (cf. Eqs. (4) and (5)). Good agreement with the model is observed when adjustable parameters given by Lin et al. [5] are applied, consistent with results reported previously for the PEGDA/PEGMEA series [5] and its shorter alkoxy-terminated analogs [9].

Conversely, the gas diffusivity does not change appreciably with co-monomer content for the PEGPEA series and decreases for the DEGPEA series, again despite the apparent increase in estimated *FFV* as co-monomer content increases in both sets of copolymers. Consequently, as shown in Figs. 12 and 13, gas diffusivity of the phenoxy-terminated copolymers does not follow the expected trends as predicted by the Cohen–Turnbull model.

An explanation for the gas diffusion behavior in phenoxy-terminated networks may lie in the polymer chain mobility, as reflected in T_g. van Amerongen found that the logarithm of gas diffusion coefficients of permanent gases in a variety of rubbery polymers depended nearly linearly on $(T-T_g)$ (i.e., the difference between the measurement temperatures and the glass transition) [20]. Certainly, in the case of the PEGDA/DEGPEA and PEGDA/PEGPEA copolymers, $(T-T_g)$ appears to be a stronger correlating factor for gas diffusivity as compared to free volume. Lin et al. [5] accounted for chain mobility effects in the PEGDA/PEGMEA system by noting that *FFV* was positively correlated with $(T-T_g)$ using Eq. (7). For the PEGDA/DEGPEA and PEGDA/PEGPEA copolymer systems, this correlation is not obeyed, i.e., *FFV* has a negative correlation with $(T-T_g)$. While insertion of the bulky phenoxy-terminated side chains seems to increase *FFV*, at the same time it also increases steric hindrance for chain motion and reduces chain mobility, as characterized by increasing T_g (cf. Fig. 5).

In a sense, the copolymers containing phenoxy-terminated side chains exhibit behavior reminiscent of glassy polymers, where insertion of functional groups into the polymer structure simultaneously increases chain stiffness and *FFV* [41,42]. For example, among substituted glassy polysulfones, tetramethyl bisphenol-A polysulfone (TMPSF) exhibits a T_g that is ∼55 °C higher than that of bisphenol-A polysulfone (PSF); TMPSF also has higher *FFV* than PSF. Transport measurements indicate gas diffusivities that are greater in TMPSF as compared to PSF [41]. In these glassy polymers,

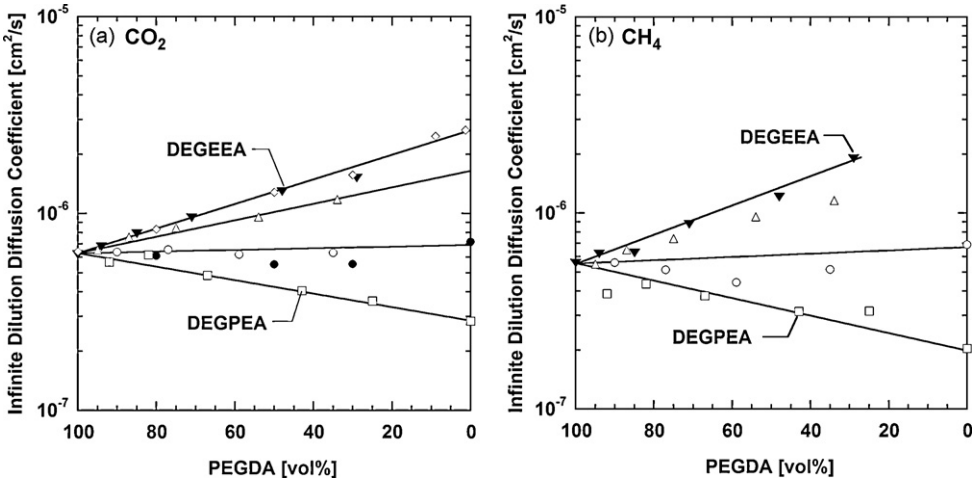

Fig. 11. Effect of PEGDA content on infinite dilution gas diffusivity at 35 °C, (a) CO_2 and (b) CH_4. The lines are drawn to guide the eye. The co-monomers are (▼) DEGEEA, (◊) PEGMEA, (△) 2-EEA, (○) PEGPEA, (□) DEGPEA, (●) PEGA. The average uncertainty is ±7% of the CO_2 diffusivity and between ±30 and ±40% of the CH_4 diffusivity.

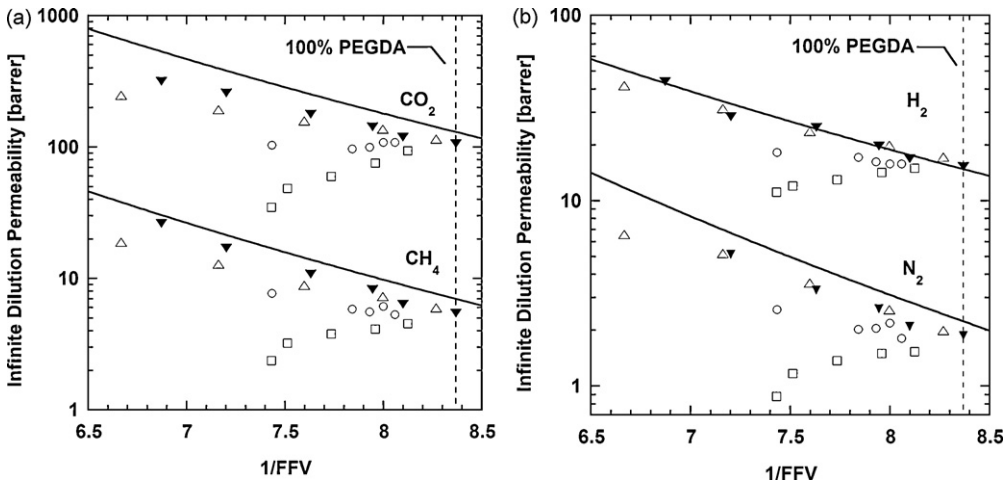

Fig. 12. Comparison between experimental and predicted infinite dilution permeability based on the free volume model, with model parameters given in Ref. [9], for (from top to bottom) (a) CO_2 and CH_4, (b) H_2 and N_2. The dashed line indicates the free volume of polymer cast from 100 wt% PEGDA in the prepolymer solution. The co-monomers of PEGDA are (▼) DEGEEA, (△) 2-EEA, (□) DEGPEA and (○) PEGPEA, with increasing content of co-monomer further away from the dashed line.

the macromolecular chains are already highly hindered, such that gas diffusivity may be influenced more strongly by increasing *FFV*, rather than by the observed variation in chain stiffness. In rubbery XLPEO with phenoxy-terminated branches, the polymer chains are fairly mobile, and the decrease in chain mobility that is a result of increasing branch content may have a stronger impact on diffusivity relative to the observed increase in *FFV*. A similar contrast is encountered when comparing the gas diffusion characteristics of (rubbery) polyethylene [PE] vs. (glassy) poly(ethylene terephthalate) [PET]. In PE, gas diffusion coefficients in the amorphous phase are substantially reduced by the presence of impermeable crystalline domains, which impose constraints on chain movement that persist into the amorphous regions [43]. In semicrystalline PET, the inherently rigid character of the PET backbone appears to be the controlling factor for chain mobility, and increasing levels of crystallinity do not significantly perturb the mobility of the amorphous phase chains [44]. As such, the gas diffusivity ascribed to the amorphous phase remains essentially constant in PET, independent of crystallinity.

An alternative explanation for the potentially disparate trends in diffusivity and permeability with *FFV* in the PEGDA/DEGPEA and PEGDA/PEGPEA systems would be that the assumptions in the *FFV* calculation for these copolymer systems are not strictly valid. Bondi's group contribution method, which was used to estimate *FFV* in this work, assumes the absence of strong non-covalent inter-chain interactions for van der Waals volume calculations [24,45,46]. Certain interactions, such as hydrogen bonding between polar groups, have been previously observed to influence the *FFV*-diffusivity correlation [9]. One possible interaction in the polymers containing phenoxy groups is localized stacking of the terminal phenyl rings as a result of π–π bond interactions, as has been proposed for the phenyl rings in benzene [47] or polystyrene [48]. In this regard, even slight differences in van der Waals volume estimates of individual functional groups could produce significant changes in the *FFV* trends [46,49]. Further, localized stacking of terminal phenyl rings could account for the decreased chain mobility that is observed, especially for the shorter DEGPEA branches. An experimental exploration of free volume characteristics in the phenoxy-terminated co-monomers may be performed using, for example, Positron Annihilation Lifetime Spectroscopy (PALS), but such studies were beyond the scope of this investigation.

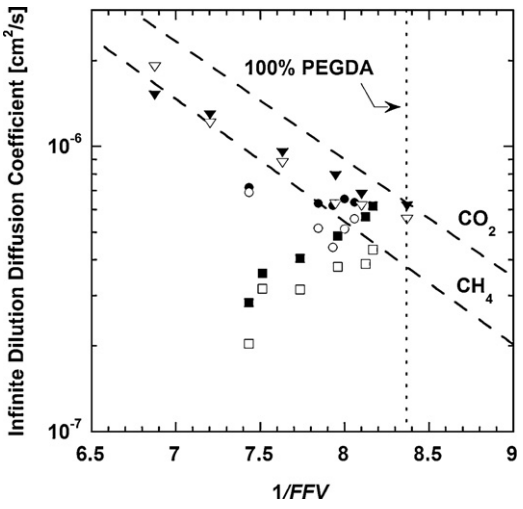

Fig. 13. Correlation between infinite dilution gas diffusivity at 35 °C and polymer free volume. The data shown are for CO_2 ((▼) PEGDA/DEGEEA, (■) PEGDA/DEGPEA and (●) PEGDA/PEGPEA) and CH_4 (analogous open symbols). The vertical dashed line indicates the free volume of polymer prepared from 100% PEGDA. The model parameters are from Ref. [9].

5. Conclusions

This study presented the influence of phenoxy-terminated side chains on the transport properties of cross-linked poly(ethylene oxide) (XLPEO) networks. Poly(ethylene glycol) diacrylate, $n = 14$ (PEGDA) was UV-polymerized with poly(ethylene glycol) phenyl ether acrylate co-monomers encompassing two different ethylene oxide repeat lengths: DEGPEA ($n = 2$) or PEGPEA ($n = 4$). These copolymer systems were compared with PEGDA networks prepared using an ethoxy-terminated co-monomer, i.e., di(ethylene glycol) ethyl ether acrylate (DEGEEA). While the introduction of phenoxy-terminated branches in XLPEGDA increased the calculated polymer fractional free volume, it did not increase gas permeability; instead, gas permeability decreased with increasing DEGPEA content and remained essentially constant at all PEGPEA concentrations. Possible explanations for these results were provided in the context of polymer chain mobility and network structure. Dynamic mechanical studies of PEGDA/PEGPEA revealed an increase in the glass transition temperature and substantial relaxation broadening with increasing PEGPEA content, despite an overall decrease in cross-link density. The PEGDA/DEGPEA networks also exhibited reduced overall chain mobility with increasing DEGPEA content, as indicated by a strong positive shift in the glass transition temperatures of the

copolymers. At the same time, dielectric measurements showed that the inclusion of phenoxy groups did not fundamentally change the local mobility of the ethylene oxide moieties. Ultimately, steric hindrance due to the phenoxy groups strongly impedes longer range segmental motion in the PEGDA/PEGPEA and PEGDA/DEGPEA materials, which was decisive in reducing gas diffusivity in these polymers. This behavior was in contrast to the PEGDA/DEGEEA networks, where fractional free volume, chain mobility and gas permeability all increased simultaneously.

Acknowledgements

We gratefully acknowledge partial support of this work by the U.S. Department of Energy (Grant DE-FG02-02ER15362) and by the U.S. National Science Foundation (Grant CBET-0515425). Activities at the University of Kentucky were supported by a grant from the Kentucky Science and Engineering Foundation as per Grant Agreement KSEF-148-502-05-130 with the Kentucky Science and Technology Corporation. The authors would like to thank Dr. Angel E. Lozano of Instituto de Ciencia y Tecnología de Polímeros (Madrid, Spain) and Dr. Donald R. Paul of the University of Texas at Austin for helpful discussions regarding some aspects of this work.

References

[1] A.L. Kohl, R.B. Nielsen, Gas Purification, 5th edition, Gulf Publishing, Houston, TX, 1997.
[2] H. Lin, B.D. Freeman, Materials selection guidelines for membranes that remove CO_2 from gas mixtures, Journal of Molecular Structure 739 (2005) 57–74.
[3] H. Lin, B.D. Freeman, Gas and vapor solubility in crosslinked poly(ethylene glycol diacrylate), Macromolecules 38 (2005) 8394–8407.
[4] H. Lin, T. Kai, B.D. Freeman, S. Kalakkunnath, D.S. Kalika, The effect of crosslinking on gas permeability in crosslinked poly(ethylene glycol diacrylate), Macromolecules 38 (2005) 8381–8393.
[5] H. Lin, B.D. Freeman, Gas permeation and diffusion in crosslinked poly(ethylene glycol diacrylate), Macromolecules 39 (2006) 3568–3580.
[6] H. Lin, E. Van Wagner, R. Raharjo, B.D. Freeman, I. Roman, High performance polymer membranes for natural gas sweetening, Advanced Materials 18 (2006) 39–44.
[7] H. Lin, E. Van Wagner, B.D. Freeman, L.G. Toy, R.P. Gupta, Plasticization-enhanced H_2 purification using polymeric membranes, Science 311 (2006) 639–642.
[8] H. Lin, E. Van Wagner, J.S. Swinnea, B.D. Freeman, S.J. Pas, A.J. Hill, S. Kalakkunnath, D.S. Kalika, Transport and structural characteristics of crosslinked poly(ethylene oxide) rubbers, Journal of Membrane Science 276 (2006) 145–161.
[9] V.A. Kusuma, B.D. Freeman, M.A. Borns, D.S. Kalika, Influence of chemical structure of short chain pendant groups on gas transport properties of cross-linked poly(ethylene oxide) copolymers, Journal of Membrane Science 327 (2009) 195–207.
[10] H. Lin, B.D. Freeman, S. Kalakkunnath, D.S. Kalika, Effect of copolymer composition, temperature, and carbon dioxide fugacity on pure- and mixed-gas permeability in poly(ethylene glycol)-based materials: free volume interpretation, Journal of Membrane Science 291 (2007) 131–139.
[11] B.D. Bhide, S.A. Stern, Membrane process for the removal of acid gases from natural gas: I. Process configurations and optimization of operating conditions, Journal of Membrane Science 81 (1993) 209–237.
[12] B.D. Freeman, I. Pinnau, Polymeric materials for gas separations, in: B.D. Freeman, I. Pinnau (Eds.), Polymer Membranes for Gas and Vapor Separation, ACS, Washington, DC, 1999, pp. 1–27.
[13] Y. Hirayama, Y. Kase, N. Tanihara, Y. Sumiyama, Y. Kusuki, K. Haraya, Permeation properties to CO_2 and N_2 of poly(ethylene oxide)-containing and crosslinked polymer films, Journal of Membrane Science 160 (1999) 87–99.
[14] M. Yoshino, K. Ito, H. Kita, K. Okamoto, Effects of hard-segment polymers on CO_2/N_2 gas separation properties of poly(ethylene oxide)-segmented copolymers, Journal of Polymer Science: Part B: Polymer Physics 38 (2000) 1707–1715.
[15] D.R. Paul, R. Clarke, Modeling of modified atmosphere packaging based on designs with a membrane and perforations, Journal of Membrane Science 208 (2002) 269–283.
[16] S. Kalakkunnath, D.S. Kalika, H. Lin, B.D. Freeman, Segmental relaxation characteristics of crosslinked poly(ethylene oxide) copolymer networks, Macromolecules 38 (2005) 9679–9687.
[17] J.H. Petropoulos, Mechanisms and theories for sorption and diffusion of gases in polymers, in: D. Paul, Yu. Yampolskii (Eds.), Polymeric Gas Separation Membranes, CRC Press, Inc., Boca Raton, FL, 1994, pp. 17–81.
[18] J.H. Dymond, K.N. Marsh, R.C. Wilhoit, K.C. Wong, Virial Coefficients of Pure Gases, 8th edition, Springer, Darmstadt, Germany, 2002.
[19] J.G. Wijmans, R.W. Baker, The solution-diffusion model: a review, Journal of Membrane Science 107 (1995) 1–21.
[20] G.J. van Amerongen, Diffusion in elastomers, Rubber Chemistry and Technology 37 (1964) 1065–1152.
[21] C.A. Kumins, T.K. Kwei, Free volume and other theories, in: J. Crank, G. Park (Eds.), Diffusion in Polymers, Academic Press, New York, 1968, pp. 107–140.
[22] H. Fujita, Diffusion in polymer–diluent systems, Fortschritte der Hochpolymeren-Forschung 3 (1961) 1–47.
[23] W.M. Lee, Selection of barrier materials from molecular structure, Polymer Engineering and Science 20 (1980) 65–69.
[24] D.W. van Krevelen, Properties of polymers: their correlation with chemical structure: their numerical estimation and prediction from additive group contributions, 3rd edition, Elsevier, Amsterdam, 1990.
[25] Yu.P. Yampolskii, Y. Kamiya, A.Yu. Alentiev, Transport parameters and solubility coefficients of polymers at their glass transition temperatures, Journal of Applied Polymer Science 76 (2000) 1691–1705.
[26] S. Kalakkunnath, D.S. Kalika, H. Lin, B.D. Freeman, Viscoelastic characteristics of U.V. polymerized poly(ethylene glycol diacrylate) networks with varying extents of crosslinking, Journal of Polymer Science: Part B: Polymer Physics 44 (2006) 2058–2070.
[27] V.I. Bondar, B.D. Freeman, I. Pinnau, Gas transport properties of poly(ether-*b*-amide) segmented block copolymers, Journal of Polymer Science: Part B: Polymer Physics 38 (2000) 2051–2062.
[28] H. Lin, B.D. Freeman, Permeation and diffusion, in: H. Czichos, L.E. Smith, T. Saito (Eds.), Springer-Handbook of Materials Measurement Methods, Springer, Berlin, 2006, pp. 371–387.
[29] V.I. Bondar, B.D. Freeman, I. Pinnau, Gas sorption and characterization of poly(ether-*b*-amide) segmented block copolymers, Journal of Polymer Science: Part B: Polymer Physics 37 (1999) 2463–2475.
[30] P.R. Bevington, D.K. Robinson, Data Reduction and Error Analysis for the Physical Sciences, 2nd edition, McGraw-Hill, Inc., New York, 1992.
[31] L.H. Sperling, Introduction to Physical Polymer Science, 3rd edition, John Wiley and Sons, Inc., New York, 2001.
[32] M.A. Borns, S. Kalakkunnath, D.S. Kalika, V.A. Kusuma, B.D. Freeman, Dynamic relaxation characteristics of crosslinked poly(ethylene oxide) copolymer networks: influence of short chain pendant groups, Polymer 48 (2007) 7316–7328.
[33] G. Williams, D.C. Watts, S.B. Dev, A.M. North, Further considerations of non symmetrical dielectric relaxation behaviour arising from a simple empirical decay function, Transactions of the Faraday Society 67 (1971) 1323–1325.
[34] S. Kalakkunnath, D.S. Kalika, H. Lin, R. Raharjo, B.D. Freeman, Molecular relaxation in cross-linked poly(ethylene glycol) and poly(propylene glycol) diacrylate networks by dielectric spectroscopy, Polymer 48 (2007) 579–589.
[35] S. Kalakkunnath, D.S. Kalika, H. Lin, R. Raharjo, B.D. Freeman, Molecular dynamics of poly(ethylene glycol) and poly(propylene glycol) copolymer networks by broadband dielectric spectroscopy, Macromolecules 40 (2007) 2773–2781.
[36] J.D. Ferry, Viscoelastic Properties of Polymers, 3rd edition, Wiley, New York, 1980.
[37] S.A. Stern, S. Fang, R.M. Jobbins, Permeation of gases at high pressures, Journal of Macromolecular Science—Physics B5 (1971) 41–70.
[38] D.R. Paul, Gas transport in homogeneous multicomponent polymers, Journal of Membrane Science 18 (1984) 75–86.
[39] D.W. Breck, Zeolite Molecular Sieves, Krieger Publishing Company, Melbourne, FL, 1974.
[40] C.P. Ribeiro Jr, B.D. Freeman, Sorption and dilation of carbon dioxide, ethane, and their mixtures in a cross-linked poly(ethylene oxide) copolymer, Journal of Membrane Science, submitted for publication.
[41] J.S. McHattie, W.J. Koros, D.R. Paul, Gas transport properties of polysulphones: 1. Role of symmetry of methyl group placement on bisphenol rings, Polymer 32 (1991) 840–850.
[42] J.S. McHattie, W.J. Koros, D.R. Paul, Gas transport properties of polysulphones: 2. Effect of bisphenol connector groups, Polymer 32 (1991) 2618–2625.
[43] A.S. Michaels, H.J. Bixler, Flow of gases through polyethylene, Journal of Polymer Science 50 (1961) 413–439.
[44] A.S. Michaels, W.R. Vieth, J.A. Barrie, Diffusion of gases in polyethylene terephthalate, Journal of Applied Physics 34 (1963) 13–20.
[45] A. Bondi, van der Waals volumes and radii, The Journal of Physical Chemistry 68 (1964) 441–451.
[46] D.H. Weinkauf, D.R. Paul, Gas transport properties of thermotropic liquid-crystalline copolyesters: II. The effects of copolymer composition, Journal of Polymer Science: Part B: Polymer Physics 30 (1992) 837–849.
[47] A.H. Narten, X-ray diffraction pattern and models of liquid benzene, Journal of Chemical Physics 67 (1977) 2102–2108.
[48] G.R. Mitchell, A.H. Windle, Structure of polystyrene glasses, Polymer 25 (1984) 906–920.
[49] J.Y. Park, D.R. Paul, Correlation and prediction of gas permeability in glassy polymer membrane materials via a modified free volume based group contribution method, Journal of Membrane Science 125 (1997) 23–39.